


 Cite this: *Chem. Commun.*, 2023, 59, 7032

 Received 7th April 2023,  
Accepted 28th April 2023

DOI: 10.1039/d3cc01729j

rsc.li/chemcomm

## Organolithium aggregation as a blueprint to construct polynuclear lithium nickelate clusters†

 Andryj M. Borys \* and Eva Hevia \*

**By exploiting the high aggregation of aliphatic lithium acetylides, here we report the synthesis and structural analysis of polynuclear lithium nickelate clusters in which up to 10 equivalents of organolithium can co-complex per Ni(0) centre. Exposure of the Ni(0)-ate clusters to dry air provides an alternative route to homoleptic Ni(II)-ates.**

The aggregation and solvation of organo-alkali-metal compounds plays a crucial role in influencing their reactivity and selectivity.<sup>1–3</sup> Typically, polar ethereal solvents such as THF or polydentate amine donors such as TMEDA (*N,N,N',N'*-tetramethylethylenediamine)<sup>4</sup> or PMDETA (*N,N,N',N',N''*-pentamethyldiethylenetriamine)<sup>5</sup> are employed to break down oligomeric aggregates into kinetically activated monomers or dimers, which exhibit enhanced reactivity, particularly towards deprotonative metalations. Contrastingly, there have been limited applications to date that take advantage of the high aggregation of organo-alkali-metal compounds. Numerous studies and reviews have been documented that assess the aggregation of organo-alkali-metal compounds in solution and the solid-state,<sup>1–3,6</sup> yet lithium acetylides are comparatively underexplored in this domain.<sup>7–9</sup> In 1987, Weiss and co-workers reported that <sup>t</sup>Bu-C≡C-Li can form THF-solvated tetrameric and dodecameric aggregates in the solid-state simply depending on the crystallisation conditions employed.<sup>10</sup> Additional factors such as London dispersion interactions may also play an overlooked role, as evidenced by the dimeric aggregate of Ph-C≡C-Li with TMPDA (*N,N,N',N'*-tetramethylpropanediamine)<sup>11</sup> versus the tetrameric aggregate of Ph-C≡C-Li with TMHDA (*N,N,N',N'*-tetramethylhexanediamine)<sup>12</sup> in which the diamine donors differ only in the backbone chain length.

Beyond their well-established applications in deprotonative metalation, metal-halogen exchange and nucleophilic addition or substitution reactions, organo-alkali-metal compounds can

also serve as anionic ligands towards a range of secondary metals (s-, p-, d- and f-block) to give rise to heterobimetallic complexes.<sup>13,14</sup> In this context, the coordination of polar organometallics to Ni(0)-olefin complexes can afford highly reactive heterobimetallic nickelates,<sup>15</sup> and we have recently assessed the rich co-complexation chemistry of Ni(COD)<sub>2</sub> (COD = 1,5-cyclooctadiene) with various organo-alkali-metal compounds such as aryl-lithiums and lithium acetylides.<sup>16–19</sup> In several cases, additional molecules of organolithium are readily incorporated within the nickelate structure, but not coordinated directly to Ni(0), and this feature has also been observed with lithium halides<sup>17</sup> and alkali-metal alkoxides.<sup>17,20</sup> Lithium nickelates with Li:Ni ratios of 1:1, 2:1 and 3:1 have now been documented,<sup>15–19</sup> and we sought to exploit the high aggregation ability of aliphatic lithium acetylides to access new classes of lithium nickelates with higher Li:Ni ratios.

We began by investigating the aggregation of <sup>t</sup>Bu-C≡C-Li in the absence of strong donor solvents or Lewis bases.<sup>8,21</sup> Crystallisation of <sup>t</sup>Bu-C≡C-Li from Et<sub>2</sub>O and pentane afforded single crystals identified as a decameric (10 units) aggregate, [Li<sub>10</sub>(Et<sub>2</sub>O)<sub>4</sub>(C≡C-<sup>t</sup>Bu)<sub>10</sub>] (1, Fig. 1). The solid-state structure consists of four linearly-fused heterocubanes in which the terminal Li atoms (Li1 and Li2) are solvated by Et<sub>2</sub>O – this bears similar structural properties to the dodecameric (12 units) aggregate reported by Weiss, [Li<sub>12</sub>(THF)<sub>4</sub>(C≡C-<sup>t</sup>Bu)<sub>12</sub>], which instead contains five linearly-fused heterocubanes despite the presence of the stronger donor solvent THF.<sup>10</sup> <sup>1</sup>H DOSY NMR spectroscopy studies support that large aggregates [Li<sub>n</sub>(THF)<sub>4</sub>(C≡C-<sup>t</sup>Bu)<sub>n</sub>] (where *n* = 10 or 12) are retained in weakly coordinating solvent systems (C<sub>6</sub>D<sub>6</sub> + 1 equiv. THF-d<sub>8</sub>), whilst in bulk THF-d<sub>8</sub>, <sup>t</sup>Bu-C≡C-Li is tetrameric (see the ESI† for more details). This is consistent with literature reports that have employed cryoscopy measurements<sup>8</sup> or low-temperature <sup>13</sup>C NMR spectroscopy in tandem with isotopic labelling to determine the aggregation of <sup>t</sup>Bu-C≡C-Li in THF solutions.<sup>7</sup>

With this knowledge in hand, we then went on to assess the reactivity of <sup>t</sup>Bu-C≡C-Li with Ni(COD)<sub>2</sub> in weakly coordinating solvent systems. Room temperature treatment of Ni(COD)<sub>2</sub>

Departement für Chemie, Biochemie und Pharmazie, Universität Bern, Bern 3012, Switzerland. E-mail: andryj.borys-smith@unibe.ch, eva.hevia@unibe.ch

† Electronic supplementary information (ESI) available: Synthetic procedures, and structural and spectroscopic data. CCDC deposition numbers: 2254773–2254780. For ESI and crystallographic data in CIF or other electronic format see DOI: <https://doi.org/10.1039/d3cc01729j>



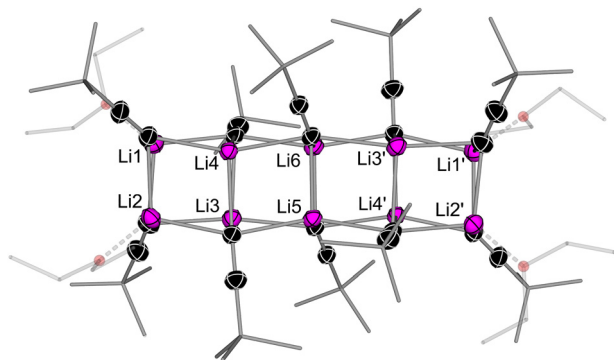


Fig. 1 Molecular structure of  $[\text{Li}_{10}(\text{Et}_2\text{O})_4(\text{C}\equiv\text{C}-t\text{Bu})_{10}]$  (**1**). Thermal ellipsoids shown at 30% probability. Hydrogen atoms omitted and  $t\text{Bu}$  groups and coordinated  $\text{Et}_2\text{O}$  shown as wireframes for clarity.

with excess  $t\text{Bu}-\text{C}\equiv\text{C}-\text{Li}$  (optimised with 9 equivalents) in  $\text{Et}_2\text{O}$  (Fig. 2a), followed by crystallisation from pentane at  $-30^\circ\text{C}$  afforded emerald green crystals identified as a solvent-free, 9 : 1 lithium nickelate cluster,  $[\text{Li}_9\text{Ni}(\text{C}\equiv\text{C}-t\text{Bu})_9]_2$  (**2**, Fig. 2b). This unique heterobimetallic cluster is constructed from three distinct building blocks (Fig. 2c): (i) a cyclotrimeric lithium acetylide ‘end cap’; (ii) a distorted-planar tri-lithium nickelate; and (iii) a cyclohexameric lithium acetylide core, which brings two nickelate units together to form a 20-metal-centred

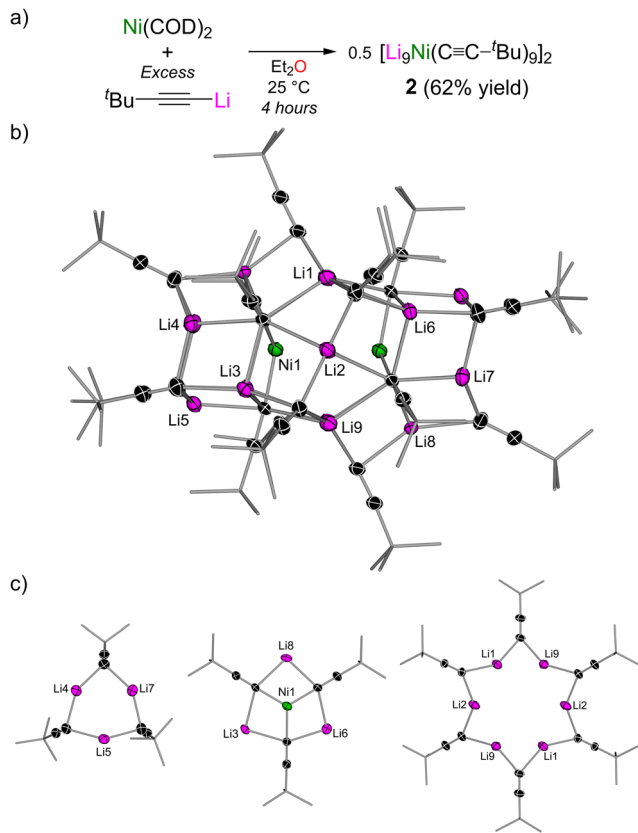


Fig. 2 (a) Synthesis of  $[\text{Li}_9\text{Ni}(\text{C}\equiv\text{C}-t\text{Bu})_9]_2$  (**2**). (b) Molecular structure of **2**. Thermal ellipsoids shown at 30% probability. Hydrogen atoms omitted and  $t\text{Bu}$  groups shown as wireframes for clarity. (c) Building blocks of **2**.

cluster. The  $\text{Li}\cdots\text{Ni}$  distances in the tri-lithium nickelate unit range from 2.64(1) to 2.654(7) Å, which is outside the sum of the covalent radii (2.52 Å)<sup>22</sup> and longer than observed in  $[\text{Li}_3(\text{TME-DA})_3\text{Ni}(\text{C}\equiv\text{C}-\text{Ph})_3]$  [2.487(4)–2.512(3) Å] in which the  $\text{Li}\cdots\text{Ni}$  interactions were found to be repulsive in nature despite their close proximity.<sup>18</sup> The three unique environments observed in the solid-state are also evidenced in the  $^1\text{H}$  NMR spectrum to give three signals of equal intensity at  $\delta$  1.79, 1.44 and 1.42. The  $^7\text{Li}$  NMR spectrum of **2** shows two signals in an approximate 1 : 2 ratio at  $\delta$  1.47 and 0.10, which can be assigned to  $[\text{Li}_3\text{Ni}(\text{C}\equiv\text{C}-t\text{Bu})_3]$  and  $[t\text{Bu}-\text{C}\equiv\text{C}-\text{Li}]_n$ , respectively (*c.f.*  $\delta$  0.52 for the free lithium acetylide).  $^1\text{H}$  DOSY NMR spectroscopy reveals that only one species exists in toluene- $d_8$  solution but suggests that  $[\text{Li}_9\text{Ni}(\text{C}\equiv\text{C}-t\text{Bu})_9]_2$  (**2**) dissociates to “ $\text{Li}_9\text{Ni}(\text{C}\equiv\text{C}-t\text{Bu})_9$ ” (see the ESI† for further details).

The absence of any coordinating solvents in the solid-state structure of **2** is particularly surprising and illustrates that the acetylide carbanion is a more suitable donor than  $\text{Et}_2\text{O}$  (both from an electronic and steric consideration), which may also explain the high aggregation of the free lithium acetylide in the absence of strong donor solvents or Lewis bases. Compound **2** is a rare example of a polynuclear organometallic cluster containing two distinct metals and to the best of our knowledge represents a new structural motif and stoichiometry in heterobimetallic ‘ate’ chemistry.

Extending this simple synthetic strategy to  $\text{Me}_3\text{Si}-\text{C}\equiv\text{C}-\text{Li}$  (optimised with 10 equivalents) (Fig. 3a) instead led to the isolation of  $\text{Li}_{10}(\text{Et}_2\text{O})_3\text{Ni}(\text{C}\equiv\text{C}-\text{SiMe}_3)_{10}$  (**3**, Fig. 3b), which grew as large orange crystals from  $\text{Et}_2\text{O}$  and  $(\text{Me}_3\text{Si})_2\text{O}$ . Unlike  $[\text{Li}_9\text{Ni}(\text{C}\equiv\text{C}-t\text{Bu})_9]_2$  (**2**), which contains two tri-lithium nickelate units, the 10 : 1 Li : Ni cluster **3** contains a single tetra-lithium nickelate core (Fig. 3c), which is decorated by six

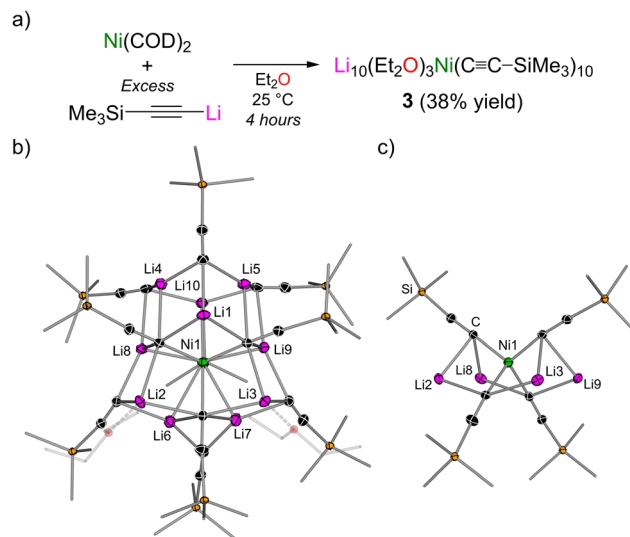


Fig. 3 (a) Synthesis of  $\text{Li}_{10}(\text{Et}_2\text{O})_3\text{Ni}(\text{C}\equiv\text{C}-\text{SiMe}_3)_{10}$  (**3**). (b) Molecular structure of **3**. Thermal ellipsoids shown at 30% probability. Hydrogen atoms and one coordinated  $\text{Et}_2\text{O}$  omitted and  $\text{Me}_3\text{Si}$  groups shown as wireframes for clarity. Only one molecule in the asymmetric unit is shown. (c) Simplified view of the tetra-lithium nickelate core of **3**.



additional lithium acetylides. This tetrahedral Ni(0)-ate motif has been proposed in the closely related  $[\text{K}_4\text{Ni}(\text{C}\equiv\text{C}-\text{H})_4]$  species, which can be obtained by potassium metal reduction of  $[\text{K}_2\text{Ni}(\text{C}\equiv\text{C}-\text{H})_4]$ .<sup>23</sup> This compound however was reported to be insoluble even in liquid  $\text{NH}_3$ , in contrast to the high hydrocarbon solubility of  $\text{Li}_{10}(\text{Et}_2\text{O})_3\text{Ni}(\text{C}\equiv\text{C}-\text{SiMe}_3)_{10}$  (**3**). Compound **3** therefore represents the first structurally characterised Ni(0) complex coordinated by four carbanions. The requirement however for the additional lithium acetylides to stabilise the “ $\text{Li}_4\text{Ni}(\text{C}\equiv\text{C}-\text{SiMe}_3)_4$ ” motif is supported by our previous reports that showed that the treatment of  $\text{Ni}(\text{COD})_2$  with 3 equivalents of  $\text{Me}_3\text{Si}-\text{C}\equiv\text{C}-\text{Li}$  in the presence of TMEDA does not give the homoleptic tri-lithium nickelate  $\text{Li}_3(\text{TMEDA})_3\text{Ni}(\text{C}\equiv\text{C}-\text{SiMe}_3)_3$  but instead gives a dinickel complex in which the lithium acetylide coordinates in a side-on fashion to modulate the electron-density at the electron-rich nickel centers.<sup>18</sup>

$^1\text{H}$  DOSY NMR spectroscopy indicates that  $\text{Li}_{10}(\text{Et}_2\text{O})_3\text{Ni}(\text{C}\equiv\text{C}-\text{SiMe}_3)_{10}$  (**3**) is fully retained in toluene- $d_8$  solution. In THF- $d_8$ , however, the lithium nickelate cluster dissociates to “ $\text{Li}_4(\text{THF})_n\text{Ni}(\text{C}\equiv\text{C}-\text{SiMe}_3)_4$ ” and the free lithium acetylide  $(\text{Me}_3\text{Si}-\text{C}\equiv\text{C}-\text{Li})_x(\text{THF})_y$ , as supported by  $^1\text{H}$  and  $^7\text{Li}$  NMR spectroscopy and confirmed by two independent species that do not co-diffuse by  $^1\text{H}$  DOSY NMR spectroscopy (see the ESI† for full details).  $^1\text{H}$  DOSY NMR spectroscopy studies on  $\text{Me}_3\text{Si}-\text{C}\equiv\text{C}-\text{Li}$  indicate that it forms lower aggregates when compared to  $^t\text{Bu}-\text{C}\equiv\text{C}-\text{Li}$  in both weakly coordinating solvent systems (hexamer) and bulk THF (dimer),<sup>24</sup> which likely influences the final lithium nickelate cluster obtained (*i.e.* 2 vs. 3).

Polynuclear transition-metal clusters are often sensitive to the crystallisation conditions employed<sup>25,26</sup> and this was also observed to be true for the lithium nickelate clusters. Whilst  $\text{Li}_{10}(\text{Et}_2\text{O})_3\text{Ni}(\text{C}\equiv\text{C}-\text{SiMe}_3)_{10}$  (**3**) was the only species that could be crystallographically identified when treating  $\text{Ni}(\text{COD})_2$  with  $\text{Me}_3\text{Si}-\text{C}\equiv\text{C}-\text{Li}$ , regardless of the stoichiometry and crystallisation conditions, the isostructural  $^t\text{Bu}-\text{C}\equiv\text{C}-\text{Li}$  analogue  $\text{Li}_{10}(\text{Et}_2\text{O})_3\text{Ni}(\text{C}\equiv\text{C}-^t\text{Bu})_{10}$  (**4**) could also be crystallographically characterised (see the ESI† for the full structure) by simply switching to  $\text{Et}_2\text{O}$  and  $(\text{Me}_3\text{Si})_2\text{O}$  as crystallisation solvents instead of pentane that was used to crystallise  $[\text{Li}_9\text{Ni}(\text{C}\equiv\text{C}-^t\text{Bu})_9]_2$  (**2**). Additionally, when treating  $\text{Ni}(\text{COD})_2$  with lower equivalents of  $^t\text{Bu}-\text{C}\equiv\text{C}-\text{Li}$  (5 equivalents), 26-metal-centred cluster  $[\text{Li}_{11}(\text{Et}_2\text{O})\text{Ni}_2(\text{C}\equiv\text{C}-^t\text{Bu})_{11}]_2$  (**5**) could be isolated and characterised by single-crystal X-ray diffraction (see the ESI† for full structure). The molecular structure of **5** shows similar features to  $[\text{Li}_9\text{Ni}(\text{C}\equiv\text{C}-^t\text{Bu})_9]_2$  (**2**) and is constructed from well-defined cyclotrimeric lithium acetylide and distorted-planar tri-lithium nickelate building blocks (see Fig. 2c), but also contains regions in which the Li cations are occupationally disordered across two or more positions. Several other aliphatic lithium acetylides were also explored; cycloalkyl (propyl, pentyl, and hexyl) lithium acetylides all gave insoluble and intractable solids however, whilst  $^i\text{Pr}-\text{C}\equiv\text{C}-\text{Li}$  (10 equivalents) afforded mixed acetylide/alkoxide cluster  $[\text{Li}_{10}(\text{Et}_2\text{O})_2\text{Ni}(\text{C}\equiv\text{C}-^i\text{Pr})_8(\text{C}\equiv\text{C}-\text{Me}_2\text{O})_2]$  (**6**), albeit in low yields (see the ESI† for the full structure). Attempts to prepare or crystallise the polynuclear lithium nickelate clusters from THF



**Scheme 1** Oxidative homocoupling of  $^t\text{Bu}-\text{C}\equiv\text{C}-\text{Li}$  catalysed by  $\text{Ni}(\text{COD})_2$  in the presence of dry air. Yields refer to spectroscopic yields determined using hexamethylbenzene as an internal standard.

were unsuccessful, supporting the crucial role of aggregation in the construction of these complexes.

Terminal acetylenes and metal acetylides can undergo homocoupling in the presence of transition-metal catalysts (*e.g.* Cu, Mn, and Fe) and oxidants to afford the corresponding 1,3-dienes.<sup>27–29</sup> Several examples using Ni-catalysts have been reported<sup>30</sup> and we therefore considered whether the simple lithium acetylide/ $\text{Ni}(\text{COD})_2$  system was also catalytically competent. Exposure of  $^t\text{Bu}-\text{C}\equiv\text{C}-\text{Li}$  to dry air in the presence of 5 mol%  $\text{Ni}(\text{COD})_2$  afforded the corresponding 1,3-diene,  $^t\text{Bu}-\text{C}\equiv\text{C}-\text{C}\equiv\text{C}-^t\text{Bu}$  in a respectable 57% yield after 2 hours (Scheme 1), whilst no homocoupling is observed in the absence of a Ni catalyst. Although lithium nickelates have been shown to be key intermediates in the  $\text{Ni}(\text{COD})_2$  catalysed cross-coupling of aryl ethers with phenyl-lithium,<sup>16</sup> no reactivity was observed under stoichiometric or catalytic conditions between **2** or **3** and 2-methoxynaphthalene.

Since a large excess of the lithium acetylide is present with respect to  $\text{Ni}(\text{COD})_2$  under these catalytic conditions, it could be hypothesised that polynuclear clusters such as  $[\text{Li}_9\text{Ni}(\text{C}\equiv\text{C}-^t\text{Bu})_9]_2$  (**2**) and  $\text{Li}_{10}(\text{Et}_2\text{O})_3\text{Ni}(\text{C}\equiv\text{C}-\text{SiMe}_3)_{10}$  (**3**) initially form and are involved in the reaction. Supporting this claim, exposure of lithium nickelate clusters **2** and **3** to dry air for 1 hour resulted in a loss of colour and oxidation to the corresponding homoleptic Ni(*n*)-ates,  $[\text{Li}_2(\text{Et}_2\text{O})\text{Ni}(\text{C}\equiv\text{C}-^t\text{Bu})_4]_2$  (**7**, 55% yield) and  $\text{Li}_2(\text{Et}_2\text{O})_2\text{Ni}(\text{C}\equiv\text{C}-\text{SiMe}_3)_4$  (**8**, 34% yield) (Fig. 4a). The consumption of residual lithium acetylide *via* oxidative homocoupling means that no additional organolithium co-complexation is observed in compounds **7** and **8**, which is in contrast to lithium nickelate clusters **2–6** (*vide supra*) and related lithium ferrates prepared *via* a salt-metathesis route using excess  $\text{Me}_3\text{Si}-\text{C}\equiv\text{C}-\text{Li}$ .<sup>31</sup>

This transformation is unique from the perspective of accessing homoleptic Ni(*n*)-ates since reported synthetic routes are often low-yielding or not possible *via* traditional salt-metathesis routes with  $\text{NiX}_2$  precursors ( $\text{X} = \text{halide}$  or acetylacetonate) due to the inherent instability of the neutral  $\text{NiR}_2$  intermediates in the absence of suitable ligands,<sup>32,33</sup> and the use of bespoke polydentate ligands is generally necessary to reliably prepare  $\text{Li}_2\text{NiR}_4$  complexes (where  $\text{R} = \text{alkyl}$  or aryl).<sup>32,34</sup> This simple oxidation route starting from a readily accessible Ni(0) precursor therefore offers an alternative route to access these heterobimetallic complexes that may find further applications in catalysis and other areas of organometallic chemistry.

Compound **7** exists as a dimer in the solid-state in which two square planar  $\text{Ni}(\text{C}\equiv\text{C}-^t\text{Bu})_4$  units are offset and rotated by  $45^\circ$  (Fig. 4b). Three unsolvated Li atoms (Li1, Li2 and Li3) are sandwiched between the two  $\text{Ni}(\text{C}\equiv\text{C}-^t\text{Bu})_4$  planes, whilst one



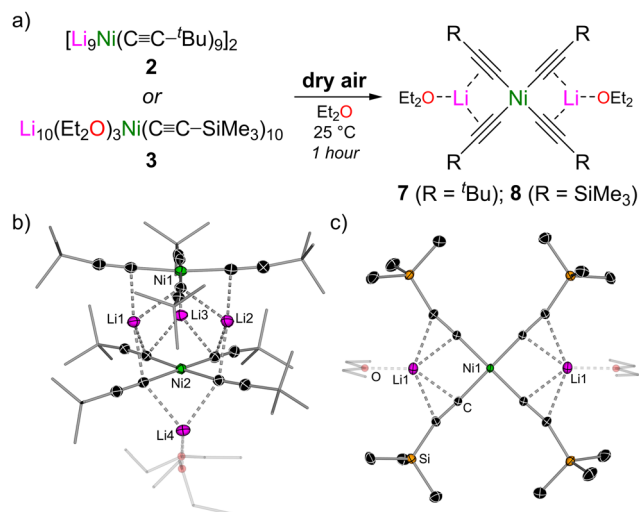


Fig. 4 (a) Synthesis of  $[\text{Li}_2(\text{Et}_2\text{O})\text{Ni}(\text{C}\equiv\text{C}-t\text{Bu})_4]_2$  (**7**) and  $\text{Li}_2(\text{Et}_2\text{O})_2\text{-Ni}(\text{C}\equiv\text{C}-\text{SiMe}_3)_4$  (**8**). (b) Molecular structure of **7**. Thermal ellipsoids shown at 30% probability. Hydrogen atoms omitted and  $t\text{Bu}$  groups and coordinated  $\text{Et}_2\text{O}$  shown as wireframes for clarity. (c) Molecular structure of **8**. Thermal ellipsoids shown at 50% probability. Hydrogen atoms omitted and coordinated  $\text{Et}_2\text{O}$  shown as wireframes for clarity.

Li atom (Li4) sits below one of the  $\text{Ni}(\text{C}\equiv\text{C}-t\text{Bu})_4$  planes and is further coordinated by two molecules of  $\text{Et}_2\text{O}$ . This asymmetric dimeric motif contrasts with  $[\text{Li}_2(\text{THF})_2\text{Ni}(\text{CH}_3)_4]_2$  that exists as a  $D_{4h}$  symmetric dimer in the solid-state where all four Li atoms are sandwiched between two  $\text{Ni}(\text{CH}_3)_4$  planes.<sup>34</sup> Despite the similar electronic and steric properties of  $t\text{Bu}$  and  $\text{Me}_3\text{Si}$ -substituents, compound **8** exists as a discrete monomer in the solid-state (Fig. 4c). The Li atoms lie in the same plane as the Ni center and four acetylide substituents and the  $\text{Li}\cdots\text{C}$  contacts adopt a narrow range [2.210(1)–2.334(2) Å vs. 2.154(3)–2.542(3) Å for **7**].

In conclusion, we have uncovered a new and structurally diverse family of polynuclear lithium nickelate clusters that can be readily accessed by treating  $\text{Ni}(\text{COD})_2$  with aliphatic lithium acetylides in  $\text{Et}_2\text{O}$  solution. Exposure of the  $\text{Ni}(0)$ -ates to dry air leads to the formation of the homoleptic  $\text{Ni}(\text{II})$ -ates with concomitant formation of the oxidative homocoupling product. This redox behaviour, along with the observation of higher order systems, hints at the possible role and applications of heterobimetallic nickelate clusters in homogenous catalysis.

We thank the SNSF (188573) and the Universität Bern for their generous sponsorship of this research.

## Conflicts of interest

There are no conflicts to declare.

## Notes and references

- 1 A. Harrison-Marchand and F. Mongin, *Chem. Rev.*, 2013, **113**, 7470–7562.
- 2 H. J. Reich, *Chem. Rev.*, 2013, **113**, 7130–7178.
- 3 V. H. Gessner, C. Däschlein and C. Strohmman, *Chem. – Eur. J.*, 2009, **15**, 3320–3334.
- 4 D. B. Collum, *Acc. Chem. Res.*, 1992, **25**, 448–454.
- 5 D. Anderson, A. Tortajada and E. Hevia, *Angew. Chem., Int. Ed.*, 2023, **62**, e202218498.
- 6 E. Hevia, M. Uzelac and A. M. Borys, *Organometallic Complexes of the Alkali Metals*, Elsevier Ltd., 4th edn, 2022.
- 7 G. Fraenkel and P. Pramanik, *J. Chem. Soc., Chem. Commun.*, 1983, 1527–1529.
- 8 W. Bauer and D. Seebach, *Helv. Chim. Acta*, 1984, **67**, 1972–1988.
- 9 A. Thompson, E. G. Corley, M. F. Huntington, E. J. J. Grabowski, J. F. Remenar and D. B. Collum, *J. Am. Chem. Soc.*, 1998, **120**, 2028–2038.
- 10 M. Geissler, J. Kopf, B. Schubert, E. Weiss, W. Neugebauer, P. von and R. Schleyer, *Angew. Chem., Int. Ed. Engl.*, 1987, **26**, 587–588.
- 11 B. Schubert and E. Weiss, *Chem. Ber.*, 1983, **116**, 3212–3215.
- 12 B. Schubert and E. Weiss, *Angew. Chem., Int. Ed. Engl.*, 1983, **22**, 496–497.
- 13 F. Mongin and A. Harrison-Marchand, *Chem. Rev.*, 2013, **113**, 7563–7727.
- 14 S. D. Robertson, M. Uzelac and R. E. Mulvey, *Chem. Rev.*, 2019, **119**, 8332–8405.
- 15 K. Jonas and C. Krüger, *Angew. Chem., Int. Ed. Engl.*, 1980, **19**, 520–537.
- 16 A. M. Borys and E. Hevia, *Angew. Chem., Int. Ed.*, 2021, **60**, 24659–24667.
- 17 R. J. Somerville, A. M. Borys, M. Perez-Jimenez, A. Nova, D. Balcells, L. A. Malaspina, S. Grabowsky, E. Carmona, E. Hevia and J. Campos, *Chem. Sci.*, 2022, **13**, 5268–5276.
- 18 A. M. Borys, L. A. Malaspina, S. Grabowsky and E. Hevia, *Angew. Chem., Int. Ed.*, 2022, **61**, e202209797.
- 19 A. M. Borys and E. Hevia, *Dalton Trans.*, 2023, **52**, 2098–2105.
- 20 K. Jonas, D. J. Brauer, C. Krüger, P. J. Roberts and Y. H. Tsay, *J. Am. Chem. Soc.*, 1976, **98**, 74–81.
- 21 A. Stasch, S. P. Sarish, H. W. Roesky, K. Meindl, F. Dall'Antonia, T. Schulz and D. Stalke, *Chem. – Asian J.*, 2009, **4**, 1451–1457.
- 22 B. Cordero, A. E. Platero-prats, M. Rev, J. Echeverr, E. Cremades and F. Barrag, *Dalton Trans.*, 2008, 2832–2838.
- 23 R. Nast and K. L. Vester, *Z. Anorg. Allg. Chem.*, 1955, **279**, 146–156.
- 24 A. C. Jones, A. W. Sanders, M. J. Bevan and H. J. Reich, *J. Am. Chem. Soc.*, 2007, **129**, 3492–3493.
- 25 R. Buschbeck, P. J. Low and H. Lang, *Coord. Chem. Rev.*, 2011, **255**, 241–272.
- 26 R. Zhang, X. Hao, X. Li, Z. Zhou, J. Sun and R. Cao, *Cryst. Growth Des.*, 2015, **15**, 2505–2513.
- 27 P. Siemsen, R. C. Livingston and F. Diederich, *Angew. Chem., Int. Ed.*, 2000, **39**, 2632–2657.
- 28 K. S. Sindhu and G. Anilkumar, *RSC Adv.*, 2014, **4**, 27867–27887.
- 29 G. Cahiez, A. Moyeux, J. Buendia and C. Duplais, *J. Am. Chem. Soc.*, 2007, **129**, 13788–13789.
- 30 M. Nasibipour, E. Safaei, M. S. Masoumpour and A. Wojtczak, *RSC Adv.*, 2020, **10**, 24176–24189.
- 31 L. A. Berben and J. R. Long, *Inorg. Chem.*, 2005, **44**, 8459–8468.
- 32 R. Taube and G. Honymus, *Angew. Chem., Int. Ed. Engl.*, 1975, **87**, 291.
- 33 H. Nakazawa, F. Ozawa and A. Yamamoto, *Organometallics*, 1983, **2**, 241–250.
- 34 D. Walther, M. Stollenz and H. Görls, *Organometallics*, 2001, **20**, 4221–4229.

